

1
2
3 **Title:** An image analysis protocol for the quantification of interglobular dentine in
4 anthropological tooth sections.
5

6
7 **Running title:** Image protocol for quantification of interglobular dentine
8

9 **Authors:** Anne Marie E. Snoddy¹, Justyna J. Miskiewicz², Carolina Loch³, Monica Tromp^{1,4},
10 Hallie R. Buckley¹.
11

12
13 **Affiliations:** 1) Department of Anatomy, University of Otago, Dunedin 2) School of
14 Archaeology and Anthropology, Australian National University, College of Arts and Sciences,
15 Canberra 3) Sir John Walsh Research Institute, Faculty of Dentistry, University of Otago,
16 Dunedin 4) Southern Pacific Archaeological Research, Archaeology Programme, School of
17 Social Sciences, University of Otago, Dunedin.
18
19
20
21
22
23
24
25
26
27
28
29
30
31
32
33
34
35
36
37
38
39
40
41
42
43
44
45
46
47
48
49
50
51
52
53
54
55
56
57
58
59
60

1
2
3 **Abstract:** The histological identification of interglobular dentine (IGD) in archaeological
4 human remains with macroscopic evidence of rickets has opened a promising new avenue
5 for the investigation of metabolic disease in the past. Recent paleopathological studies have
6 shown that histological analysis of archaeological human teeth may allow the identification
7 of periods of vitamin D deficiency occurring within very narrow developmental windows,
8 yielding new information on the seasonality or even maternal-fetal transmission of this
9 disease. However, currently available techniques for recording IGD rely on subjective
10 scoring systems or visual estimations, potentially leaving them open to inter and intra-
11 observer error rendering comparisons of datasets difficult. Here we describe a new imaging
12 protocol that utilizes open access software to yield comparatively objective and quantitative
13 data on the amount of IGD present within a dentinal region of interest. We demonstrate
14 that grayscale histograms in FIJI®/ImageJ® can be used to provide less subjective estimates
15 of the percentage of a region of interest affected by IGD. Application of this technique may
16 enable more accurate comparison of datasets between researchers.
17
18
19
20
21
22
23
24
25
26
27
28
29
30

31 **Keywords:** dental histology, vitamin D deficiency, ImageJ®, paleopathology
32
33
34
35
36
37
38
39
40
41
42
43
44
45
46
47
48
49
50
51
52
53
54
55
56
57
58
59
60

1. Introduction

Interglobular dentine (IGD) is a developmental defect in teeth, comprised of arc-shaped regions of poorly mineralized dentine bordered by unfused calcospherites (Nanci, 2018). Animal experimental studies have shown that IGD can occur during enamel maturation, and can coincide with odontoblast retraction in the dentine tubules as part of normal dental development (e.g. Kagayama et al., 1997; Tsuchiya et al., 2002). Research using modern human teeth has also noted that IGD is distributed unevenly across the root and the crown, because of regional tooth differences in the retraction of odontoblast processes (Jayawardena et al., 2009). However, a clinical association has been demonstrated between a greater presence of IGD and both inherited and acquired mineralization disorders such as familial hypophosphatemic and nutritional rickets (Seow et al., 1989; Shellis, 1983; Tracy et al., 1971). IGD has also been histologically observed in paleopathological examples of individuals with macroscopic evidence of rickets (D'Ortenzio et al., 2016; Veselka et al., 2019). In recent years, histological analysis of IGD from archaeological individuals has received increased attention due to its potential to provide evidence of vitamin D deficiency (VDD) occurring during discrete developmental periods that are too subtle or brief to manifest macroscopically (Brickley et al., 2019; Colombo et al., 2018; D'Ortenzio et al., 2016).

To date, both clinical and anthropological methods of estimating the severity of IGD formation have involved either subjective scoring systems (Mellanby, 1934; Isokawa et al., 1963) or visual estimation of the percentage of dentine tissue affected within a region of interest (ROI) (D'Ortenzio et al., 2016; Veselka et al., 2019). These methods are subjective and open to high degrees of both inter and intra-observer error, because they rely on an approximate estimation of the extent to which IGD occurs in a given tooth area. In particular, methods that estimate percentage of IGD can be ambiguous as it is difficult to identify whether they concern the proportion of dentinal tissue containing IGD only or the cumulative value of the voids created by unmineralized calcospherites (e.g. D'Ortenzio et al., 2016: 157-8). Although D'Ortenzio and colleagues have accounted for some observational variation by creating broad severity grades (e.g. grade 2 = 25-50%), we believe a more quantitative approach would be beneficial, especially when comparing datasets.

1
2
3 These recent histological reports examining IGD in archaeological samples are pioneering
4 (e.g. Brickley et al., 2019; D'Ortenzio et al., 2016; Veselka et al., 2019) and have contributed
5 greatly to the study of metabolic bone disease in past populations. However, as with all
6 developing methodologies, it is important to work towards more objective techniques that
7 reduce the potential for observational error. The aim of this technical note is to outline an
8 image analysis protocol for quantifying IGD which reduces the potential for inter and intra-
9 observer error. We use the open-access software FIJI[®], which is a version of ImageJ[®] (v.
10 1.52) that includes preinstalled plugins useful for scientific image analysis. This software is
11 commonly used in the analysis of microscopic tissue images (Schneidelin et al., 2012).

21 **2. The protocol: Grayscale Histograms in FIJI[®]**

22
23
24
25 The following is a protocol summary for calculating the percentage of a ROI within primary
26 dentine which is composed of IGD defects. The full protocol, with corresponding
27 screenshots of each step, is provided in the supplementary material. To begin, download
28 FIJI[®] and import your slide scan into the FIJI/ImageJ[®] (v. 1.52) window. Convert the image to
29 grayscale (8 bit). Use the line segment tool and trace scale bar in scanned image to set scale
30 in mm. Add grid overlay from the plugins tab; this will need to be downloaded separately
31 and installed in FIJI (see supplementary materials). Set your grid boxes to 0.5 mm². Use the
32 rectangle tool to select the area within a grid box of interest. Cut this area out into a
33 separate file. Threshold this new image to reduce background noise (variation in contrast
34 unrelated to IDG) ensuring that the IGD in new image matches IGD from the original image.
35 Regions of true IGD should appear as purely black voids. Quantify IGD by copying pixel data
36 into an Excel spreadsheet, and calculating percentage of IGD:

$$47 \quad \text{(\#black pixels/\# white pixels) x 100 = \% ROI with IGD}$$

48
49
50
51
52 The core technical principle of our protocol is the generation of grayscale histograms
53 from dental histology images. Grayscale histograms are often used in research that deals
54 with estimation of skeletal tissue density or mineralization changes (Dias et al., 2011;
55 Palacio-Mancheno et al., 2014; Wuang et al., 2014). This involves analyzing the distribution
56 of gray value pixels within an image or a specific ROI. IGD can be visualized microscopically
57
58
59
60

1
2
3 in unstained thin sections as darker, irregular voids within globular dentine areas (Nanci,
4 2018; Figure 1). By converting a high resolution slide-scan image to 8-bit grayscale and
5 increasing the contrast, the IGD voids become enhanced as regions of black pixels against
6 white background (Figure 2). The grid overlay plugin (Rasband, 2016) can be used to divide
7 the image into identically sized areas from which a single ROI can be isolated, ensuring
8 greater consistency across multiple samples (provided the same scale is used each time).
9 Running the histogram analysis function in the Fiji® software will produce a total number of
10 black and white pixels on the grayscale. These can then be used to calculate the “true”
11 percent of IGD in the ROI. The resulting percentages become quantitative data rather than
12 estimated percentage categories. The application of our protocol to an image shown in
13 D’Ortenzio et al., 2016 (p. 157, Figure 4c therein) results in an IGD count of only ~6.5%,
14 while the authors give this a visual estimate of 25-50% coverage (“grade 2”). Therefore, it is
15 clear that the severity categories provided in previous publications might have over-
16 estimated IGD presence.
17
18
19
20
21
22
23
24
25
26
27
28
29

30 **3. Methodological considerations**

31
32 In order for this protocol to be effective, the following issues need to be considered:
33
34
35

- 36
37
38 • Defects in the histological slide, such as air bubbles and artefacts from mounting or
39 embedding, will need to be erased from the scanned image prior to running the
40 histogram; otherwise, they risk artificially enhancing the IGD count. This can be
41 achieved by using the color picker tool to choose a neutral background color to
42 match the unaffected dentine and then coloring in the bubble or artefact with the
43 paintbrush tool.
44
45
- 46 • Analysis of regions of dentine with naturally high color contrast, such as those
47 containing dead tracts or reparative dentine, should be avoided as these will
48 influence the grayscale histogram.
49
50
- 51 • The grid from which ROIs are derived must be set to a standard across all images in
52 the dataset. For our analyses here, we have chosen a 0.5x0.5mm² grid at 40x
53 magnification.
54
55
56
57
58
59
60

- Histological sections compared must be of a uniform thickness (Bromage & Werning, 2013). Because IGD defects can super-impose when viewed two-dimensionally, variation in section thickness may influence the amount of dentine exposed. For example, portions of IGD located closer to the bottom surface of the thin section will appear blurred and distanced if the image was taken with a microscope objective focused on the most superior/superficial surface of the section.
- Where possible, slide imaging should be undertaken using a “z-stacking” option, so that multiple images in the z-plane are combined and flattened. This increases the depth of field of the image.

4. Conclusions

We have reported a quantitative method of recording IGD in archaeological samples of human teeth. This protocol uses freely available software and provides a means to reduce inter and intra-observer error that will facilitate comparison of datasets between research groups going forward. More work is needed in order to provide an evidence-based threshold for identifying IGD as ‘pathological’. Additional research is also needed to determine whether factors such as variation in section direction, section thickness, or the region of tooth observed (e.g. crown vs. root) influence the amount of IGD recorded. This protocol offers a first step for methodological improvement in this research area.

Data Availability Statement

The data that support the findings of this study are available from the corresponding author upon request.

Works Cited

Brickley, M. B., Kahlon, B., & D’Ortenzio, L. (2019). Using teeth as tools: Investigating the mother–infant dyad and developmental origins of health and disease hypothesis using

1
2
3 vitamin D deficiency. *American Journal of Physical Anthropology*, 25(3), 95–12.

4 <http://doi.org/10.1002/ajpa.23947>
5
6
7

8 Bromage T & Werning S. 2013. Image Standardization in Paleohistology. In Padian, K., &
9 Lamm, E. T. (Eds.). (2013). *Bone Histology of Fossil Tetrapods: Advancing Methods, Analysis,*
10 *and Interpretation*. University of California Press. p. 161-176
11
12
13
14

15 Colombo, A., D’Ortenzio, L., Bertrand, B., Coqueugniot, H., Knüsel, C. J., Kahlon, B., &
16 Brickley, M. (2018). Micro-computed tomography of teeth as an alternative way to detect
17 and analyse vitamin D deficiency. *Journal of Archaeological Science: Reports*, 23, 390–395.
18
19
20
21 <http://doi.org/10.1016/j.jasrep.2018.11.006>
22
23
24

25 Dias, G. J., Cook, R. B., & Mirhosseini, M. (2011). Influence of food consistency on growth
26 and morphology of the mandibular condyle. *Clinical Anatomy*, 24(5), 590-598.
27
28
29 <https://doi.org/10.1002/ca.21122>
30
31

32 D’Ortenzio, L., Ribot, I., Raguin, E., Schattmann, A., Bertrand, B., Kahlon, B., & Brickley, M.
33 (2016). The rachitic tooth: A histological examination. *Journal of Archaeological Science*, 72,
34 152–163. <http://doi.org/10.1016/j.jas.2016.06.006>
35
36
37
38

39 Isokawa S., Kosakai T., & Kajiyama, S. (1963). Interglobular dentin in the deciduous tooth.
40 *Journal of Dental Research*, 42, 831-834. <https://doi.org/10.1177/00220345630420031301>
41
42
43
44

45 Jayawardena, C., Nandasena, T., Abeywardena, A., & Nanayakkara, D. (2009). Regional
46 distribution of interglobular dentine in human teeth. *Archives of Oral Biology*, 54(11), 1016-
47 1021. <https://doi.org/10.1016/j.archoralbio.2009.09.001>
48
49
50
51

52 Kagayama, M., Zhu, J. X., Sasano, Y., Sato, H., & Mayanagi, H. (1997). Development of
53 interglobular dentine in rat molars and its relation to maturation of enamel. *Anatomy and*
54 *Embryology*, 196(6), 477-483. <https://doi.org/10.1007/s004290050115>
55
56
57
58
59
60

1
2
3 Mellanby, M. T. (1929). The Influence of Diet on the Structure of Teeth. *Physiological*
4 *Reviews*, 8(4), 545–577. <https://doi.org/10.1152/physrev.1928.8.4.545>
5
6
7

8
9 Tsuchiya, M., Sasano, Y., Kagayama, M., & Watanabe, M. (2002). The extent of odontoblast
10 processes in the dentin is distinct between cusp and cervical regions during development
11 and aging. *Archives of Histology and Cytology*, 65(2), 179-188.
12
13 <https://doi.org/10.1679/aohc.65.179>
14
15
16

17
18 Nanci, A. (2018). *Ten Cate's Oral histology: Development, Structure, and Function*. St. Louis,
19 Missouri: Elsevier.
20
21
22

23
24 Palacio-Mancheno, P. E., Larriera, A. I., Doty, S. B., Cardoso, L., & Fritton, S. P. (2014). 3D
25 assessment of cortical bone porosity and tissue mineral density using high-resolution μ CT:
26 Effects of resolution and threshold method. *Journal of Bone and Mineral Research*, 29(1),
27 142-150. <https://doi.org/10.1002/jbmr.2012>
28
29
30

31
32 Rasband, W. (2016). *Grid Overlay*. Retrieved from: [https://imagej.nih.gov/ij/plugins/graphic-](https://imagej.nih.gov/ij/plugins/graphic-overlay.html)
33 [overlay.html](https://imagej.nih.gov/ij/plugins/graphic-overlay.html)
34
35
36

37
38 Seow, W. K., Romaniuk, K., & Sclavos, S. (1989). Micromorphologic features of dentin in
39 vitamin D-resistant rickets: Correlation with clinical grading of severity. *Pediatric Dentistry*,
40 11(3), 203–208.
41
42
43

44
45 Schindelin, J., Arganda-Carreras, I., Frise, E., Kaynig, V., Longair, M., Pietzch, T., et al. (2012).
46 Fiji: an open-source platform for biological-image analysis. *Nature Methods*, 9(7), 676–682.
47
48 <http://doi.org/10.1038/nmeth.1985>
49
50
51

52
53 Shellis, R. P. (1983). Structural organization of calcospherites in normal and rachitic human
54 dentine. *Archives of Oral Biology*, 28(1), 85–95. [http://doi.org/10.1016/0003-](http://doi.org/10.1016/0003-9969(83)90030-4)
55 [9969\(83\)90030-4](http://doi.org/10.1016/0003-9969(83)90030-4)
56
57
58
59
60

1
2
3 Tracy, W. E., Steen, J. C., Steiner, J. E., & Buist, N. R. M. (1971). Analysis of dentine
4 pathogenesis in vitamin D-resistant rickets. *Oral Surgery, Oral Medicine, and Oral Pathology*,
5 32(1), 38–44. [http://doi.org/10.1016/0030-4220\(71\)90248-9](http://doi.org/10.1016/0030-4220(71)90248-9)
6
7
8

9
10 Veselka, B., Brickley, M. B., D'Ortenzio, L., Kahlon, B., Hoogland, M. L. P., & Waters Rist, A. L.
11 (2019). Micro-CT assessment of dental mineralization defects indicative of vitamin D
12 deficiency in two 17th–19th century Dutch communities. *American Journal of Physical*
13 *Anthropology*, 169(1), 122–131. <http://doi.org/10.1002/ajpa.23819>
14
15
16
17

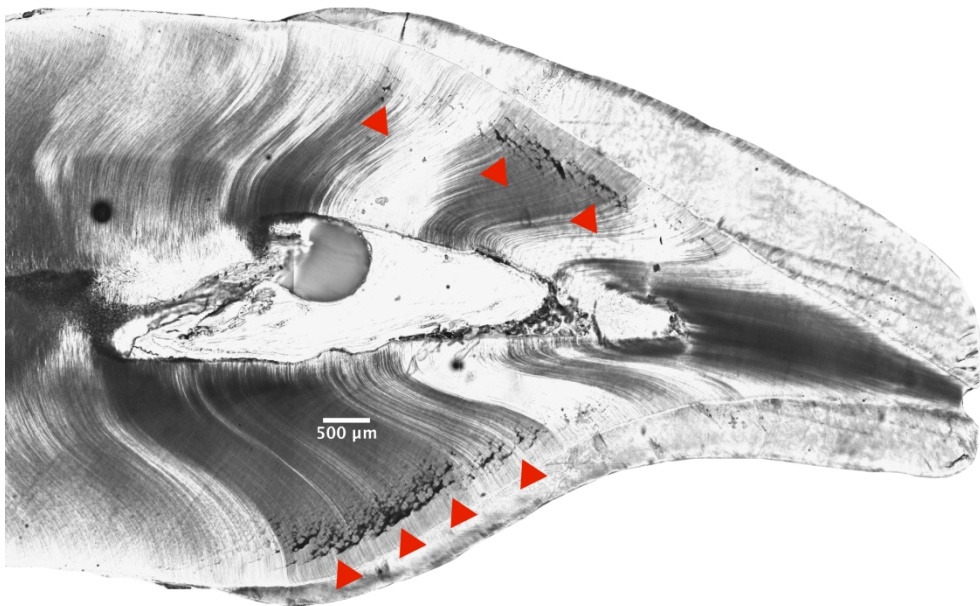
18
19 Waung, J. A., Maynard, S. A., Gopal, S., Gogakos, A., Logan, J. G., Williams, G. R., & Bassett, J.
20 H. D. (2014). Quantitative X-ray microradiography for high-throughput phenotyping of
21 osteoarthritis in mice. *Osteoarthritis and Cartilage*, 22(10), 1396–1400.
22 <https://doi.org/10.1016/j.joca.2014.04.015>
23
24
25
26
27
28
29
30
31
32
33
34
35
36
37
38
39
40
41
42
43
44
45
46
47
48
49
50
51
52
53
54
55
56
57
58
59
60

Figure Captions

Figure 1: Labio-lingual thin section of lateral mandibular incisor. Red arrows indicate areas of IGD which appear as black voids.

Figure 2: An overview of the image analysis workflow in FIJI®. (A) shows the threshold filter dialogue box. A grayscale image before applying contrast can be seen on the left (B). A grayscale histogram in ImageJ® (v 1.52) revealing IGD as regions of black pixels can be seen on the right (D). The histogram window (E) shows the grayscale distribution (0-255) with 0 indicating white pixels, and 255 indicating black pixels.

1
2
3
4
5
6
7
8
9
10
11
12
13
14
15
16
17
18
19
20
21
22
23
24
25
26
27
28
29
30
31
32
33
34
35
36
37
38
39
40
41
42
43
44
45
46
47
48
49
50
51
52
53
54
55
56
57
58
59
60



Labio-lingual thin section of lateral mandibular incisor. Red arrows indicate areas of IGD which appear as black voids.

215x143mm (300 x 300 DPI)

1
2
3
4
5
6
7
8
9
10
11
12
13
14
15
16
17
18
19
20
21
22
23
24
25
26
27
28
29
30
31
32
33
34
35
36
37
38
39
40
41
42
43
44
45
46
47
48
49
50
51
52
53
54
55
56
57
58
59
60

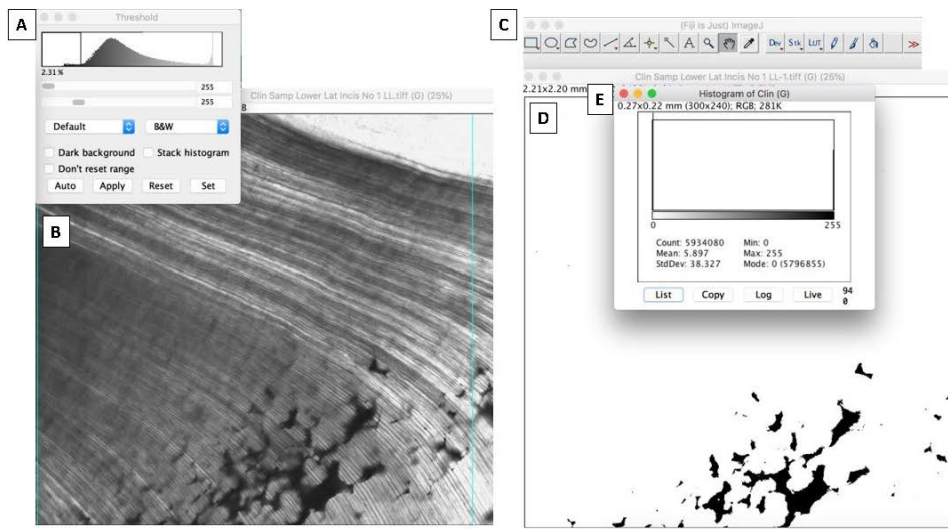


Figure 2: An overview of the image analysis workflow in FIJI®. (A) shows the threshold filter dialogue box. A grayscale image before applying contrast can be seen on the left (B). A grayscale histogram in ImageJ® (v 1.52) revealing IGD as regions of black pixels can be seen on the right (D). The histogram window (E) shows the grayscale distribution (0-255) with 0 indicating white pixels, and 255 indicating black pixels.

336x187mm (85 x 85 DPI)